Arch. Metall. Mater., Vol. 61 (2016), No 2, p.665–670

DOI: 10.1515/amm-2016-0113

A. MRÓZ*,#, D. GARBIEC*, A. WIELOWIEJSKA-GIERTUGA*, T. WIŚNIEWSKI*, M. GIERZYŃSKA-DOLNA*, A. MARTYŁA**

STRUCTURAL, MECHANICAL AND TRIBOLOGICAL PROPERTIES OF SPARK PLASMA SINTERED Ti6Al4V ALLOY

The influence of spark plasma sintering parameters on the structural, mechanical and tribological characteristics of the Ti6Al4V alloy, which is used as implant material in biomedical engineering, was investigated. The experimental data confirm that full density and attractive mechanical properties can be obtained using the spark plasma sintering method. Tribological tests, performed in dry conditions, allowed the authors to indicate the most suitable sintering parameters. The material characterized by the highest wear resistance was selected for further tribological testing in articulation with UHMWPE in simulated body fluids. Although the weight of the polymeric material articulating against the sintered Ti6Al4V was slightly higher compared to the UHMWPE articulating against the reference material (Ti6Al4V rod), the friction coefficient was lower.

Keywords: Ti6Al4V alloy, spark plasma sintering, mechanical properties, friction and wear properties

1. Introduction

The Ti6Al4V alloy was discovered in 1954 through the addition of 6% aluminum to titanium to stabilize the α phase and 4% vanadium to stabilize the β phase [1]. Thanks to this, an alloy with favorable mechanical properties and good biocompatibility was obtained. This material is currently widely used for both porous and solid implants (artificial hip or knee-joints). For the first group the main problem is deformation and fracture behavior [2], while for the second group tribological behavior and long-term stability are challenges [3]. Moreover, due to its high melting temperature and extreme chemical affinity to gaseous atmospheres (e.g. oxygen, hydrogen, nitrogen), particularly at elevated temperatures, certain difficulties may arise when sintering this material [1]. Thus, there is growing interest in new powder metallurgy methods such as spark plasma sintering [4]. Studies on the Ti6Al4V alloy produced by the SPS method have been undertaken in many research centers around the world. Open literature indicates that SPS processes have been performed at temperatures ranging from 700 to 1500°C and compaction pressures ranging from pressureless to 80 MPa. A heating rate of 100°C/min and a holding time ranging from 2.5 to 20 minutes have also been applied [1, 4-7]. The goal of the present research was to study the influence of sintering temperature and compaction pressure on the mechanical and tribolocal properties of the Ti6Al4V alloy sintered using the SPS method destined for long-term implants.

2. Materials and methods

In order to fabricate the sintered materials Ti6Al4V powder (Kamb Import-Export, Poland, particle size 20-63 μm, 99.9% purity) with a fine spherical morphology was densified using a spark plasma sintering HP D 25-3 furnace (FCT, Germany). The powder was heated up to 1200 and 1300°C at 100°C/min in vacuum of 5 Pa and held at the sintering temperature for 2.5 min. The pressure level on the specimens was kept constant at 25 and 50 MPa throughout the sintering process. The temperature was monitored by an optical pyrometer throughout a non-through hole in the graphite upper punch. From spark plasma sintered Ti6Al4V compacts with dimensions of Ø40x10 mm, samples for tests were cut by the wire electrical discharge machining.

The sintered materials were evaluated for their microstructure, phase analysis and mechanical properties. The phase analysis was conducted with a PW 1050 (Philips, The Netherlands) powder diffractometer with CuKα radiation (λ = 1.54060 Å). The microstructure was observed with the use of an Eclipse L150 (Nikon, Japan) light microscope. The density of the specimens was measured by means of the Archimedes method. Vickers microhardness was measured according to the ISO 6507-1:2007 standard with the use of a MICROMET 2104 (Wirtz-Buehler, Germany) and applying a load of 0.4903 N for 15 s. The compressive strength was measured without lubricant using a 4483 Instron mechanical testing machine of the measuring range of up to 150 kN (constant crosshead speed) with the initial strain rate of 0.0033 s^{-1}. For the tests, samples with dimensions of Ø10x10 mm were used. Comparative preliminary tribological tests were performed using a "block-on-ring" tribometer (Institute for Sustainable Technologies – National Research Institute, Poland). The tests were carried out according to ASTM G77 under dry conditions. 100Cr6 steel rings of sizes 35 mm × 6 mm were driven to rotate against stationary upper blocks (sintered material) of a size 15.7 mm × 10 mm × 6

* METAL FORMING INSTITUTE, POZNAN, POLAND

** CENTRAL LABORATORY OF BATTERIES AND CELLS, POZNAN, POLAND

Corresponding author: adren.mroz@inop.poznan.pl

mm (non-conformal contact) at a linear velocity of 0.36 m/s (200 rpm), a load of 220 N (initial tension stress of 406 MPa), and duration of 46 min (a sliding distance of 1000 m). A characteristic feature of the used test combination is that the surface area of contact between the sample and the counterbody constantly increases in a nonlinear manner during the test. The greater susceptibility to wear, the greater the contact area. If the tribological properties of the materials compared with each other are different but similar, the use of such a system can more reliably indicate which one has greater resistance to wear on a relatively short friction path (readability). However, it should be kept in mind that the wear indicators in such a case are unreliable and should not be compared.

The tests were repeated three times for each sintered material. On the basis of the above-described methodology, the sintered materials characterized by the best tribological properties were identified.

In the second stage, a "pin-on-plate" tribometer (Institute for Sustainable Technologies – National Research Institute, Poland) was applied. The tests were run according to ASTM F732. Wear pins (made of UHMWPE, ISO 5834-1+2) were articulated against smooth metallic plates of a diameter of 36 mm made of the best sintered material from the tribological point of view and reference material - Ti6Al4V rod, ISO 5832-3). The tests were carried out under standard kinematic conditions, under a load of 200 N (nominal contact pressure 3.21 MPa) during 1 000 000 cycles at 1 Hz and with a stroke length of 25 mm. The tests were carried out at the temperature of 37 ± 3°C. As a lubricant a 20% water solution of bovine serum was used. In accordance to the ISO 14242-1 standard, the fluid test medium was filtered through a 22 μm filter and has a protein mass concentration of 20 g/l. To minimize the microbiological concentration, the fluid test medium was stored frozen (temperature of -20°C) until required for testing. An antimicrobial reagent – sodium azide 0.3% (Aldrich Chemistry Co. LLC, Germany) was added. Polymer pins were soaked in the lubricant for 48 hours in a controlled environment to stabilize the material. Before weighing both before and after the tests, the samples were cleaned and dried in accordance to the ISO 14242-2 standard. During the cleaning process an ultrasonic cleaner as well as following liquids: distilled water, isopropyl alcohol and detergent were used. The metallic samples were weighed using a digital balance R200D (Sartorius, Germany), the polymer ones using a digital micro-balance 4503 MICRO (Sartorius, Germany). The roughness measurements of the bearing surfaces were determined with the use of a Hommel Etamic T8000RC profilometer (Jenoptik AG, Germany). The worn surface morphologies of the samples were examined under SEM Inspect S, (FEI, The Netherlands) to assist the analysis of the wear mechanisms.

3. Results and discussion

Fig. 1 presents the X-ray spectra of the Ti6Al4V powder and spark plasma sintered Ti6Al4V. The α-Ti (hcp) and β-Ti (bcc) phases are present in all the sintered materials. By comparing the spectra of the powder material with those of the spark plasma sintered materials, a slight shift of peaks in the direction of lower counts can be observed, which is caused by the presence of the β-Ti phase and has been confirmed by other authors [8,9]. Additionally, the presence of the β-Ti phase increases with an increasing sintering temperature and is reflected in the intensity of the β-Ti (211) peak. Changes during sintering are reflected in the parameters of the elementary cell as well. A data compilation is given in TABLE 1.

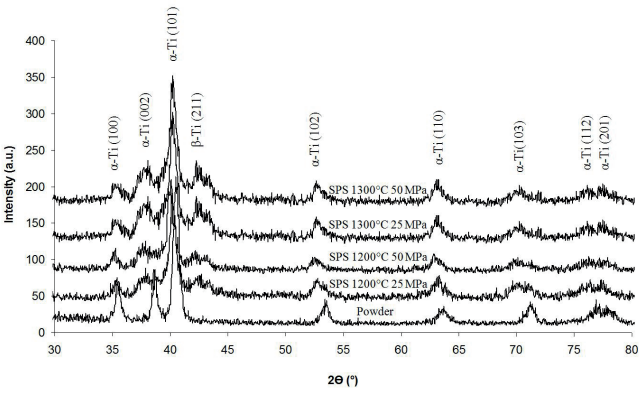

Fig. 1. X-ray spectra of powder and spark plasma sintered Ti6Al4V

TABLE 1
Elementary cell parameters of powder and spark plasma sintered Ti6Al4V

	a (Å)	c (Å)	V (Å^3)
Powder	2.930	4.658	34.590
SPS: 1200°C 25 MPa	2.938	4.757	35.518
SPS: 1200°C 50 MPa	2.943	4.789	35.857
SPS: 1300°C 25 MPa	2.934	4.799	35.734
SPS: 1300°C 50 MPa	2.882	4.647	33.390

Fig. 2 shows the microstructures of spark plasma sintered Ti6Al4V at various temperatures and compaction pressures. In all the cases, the sintered materials are characterized by a lamellar α/β structure with α' separation formed during rapid cooling. Dabrowski reported that β → α' + α transformation occurred during cooling Ti6Al4V alloys from 7.3 to 23.1°C/s [10]. In addition, there is a clearly visible difference in the α/β grain size among the materials sintered at various sintering temperatures and compaction pressures. In this study, the grains grow with an increasing sintering temperature from 1200 to 1300°C. Moreover, during the spark plasma sintering process at 25 MPa, the grains grow significantly up to approx. 500 μm. Doubling the compaction pressure (from 25 to 50 MPa) causes limitation of this phenomenon, which in open literature is not fully explained and therefore needs to be further investigated.

The results of the density measurements, Vickers microhardness measurements and compressive strength measurements are presented in TABLE 2. It can be concluded from analysis of the obtained results that an increase in sintering temperature has a slight effect of increasing the relative density of the studied materials. The compaction pressure effect was secondary. The sintered materials produced at a temperature of 1300°C under a compaction pressure of 50 MPa exhibited the highest density (4.44 g/cm^3).

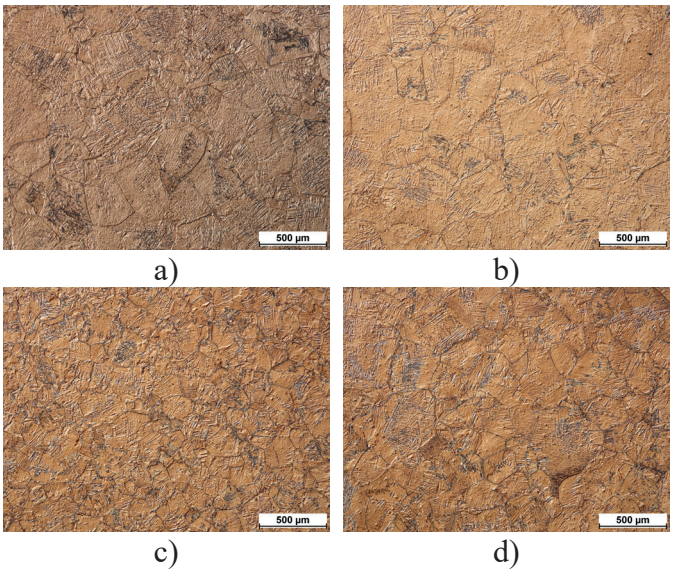

Fig. 2. Spark plasma sintered Ti6Al4V microstructures: a) 1200°C and 25 MPa, b) 1300°C and 25 MPa, c) 1200°C and 50 MPa, d) 1300°C and 50 MPa

From the performed tests, it is seen that an increase in the sintering temperature from 1200 to 1300°C does not cause spectacular changes in the microhardness of the studied materials. An increase in compaction pressure from 25 to 50 MPa has the effect of reducing the microhardness of the obtained materials on average by 6% for the temperature of 1200°C, and on average by 4.5% for the temperature of 1300°C. The sintered materials fabricated with the compaction pressure of 25 MPa are characterized by the highest microhardness (above 300 HV0.05).

Fig. 3 shows the compressive stress-strain curves of the spark plasma sintered Ti6Al4V alloy at various sintering temperatures and compaction pressures. The stress-strain curves show the typical elastic and plastic deformation. An increase in sintering temperature and compaction pressure does not cause significant changes in the compressive strength of the spark plasma sintered Ti6Al4V alloy (TABLE 2). The greatest compression strength (1159 and 1166 MPa) was obtained by the sintered materials produced at a compactive pressure of 50 MPa. Based on a performed static compressivetest, it was found that these materials are characterized by a ductility of ~22%. The Ti6Al4V alloy produced using the SLM method is distinguished by a similar compressive strength [11]. The least deformation (~19%) was obtained for the sintered material with the lowest compressive strength (1150 MPa), produced at a temperature of 1300°C and under a compaction pressure of 25 MPa.

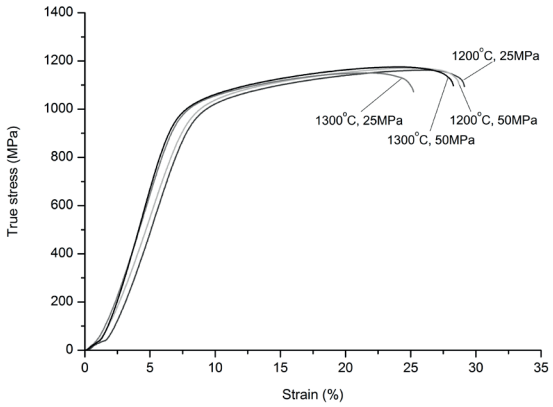

Fig. 3. Stress-strain curves of spark plasma sintered Ti6Al4V

The relations between the applied parameters during spark plasma sintering and the friction coefficient, the wear resistance as well as the Ra roughness for the tested tribocouples are presented in TABLE 3. The initial roughness of the tested samples was varied, despite the fact that the grinding procedure was the same. The correlation between the sintering temperature and the compaction pressure can be easily seen, both before and after the tribological tests. The R_a parameter decreases with increasing temperature and increasing compaction pressure (TABLE 3). The wear resistance, in a similar way to the roughness, depends on the spark plasma sintering parameters. The weight loss decreases with increasing sintering temperature and increasing compaction pressure (TABLE 4). For example, the Ti6Al4V samples sintered at the temperature of 1300°C under 50 MPa were characterized by the highest wear resistance. The average weight loss of those blocks was 40% lower in comparison to the materials sintered at the temperature of 1300°C under 25 MPa – the worst material from the tribological point of view. Moreover, the lowest median friction coefficient ranging from 0.34 - 0.36 (complete range 0.21 - 0.54) was identified under dry conditions for the material sintered at the temperature of 1300°C with the compaction pressure of 50 MPa. A significant variation in weight loss might be a factor of mutual participation of the α-Ti and β-Ti phases, which confirm the XRD results. If the presence of β-Ti increases, the wear resistant increases. Similar conclusions were reached by the authors of [12], who studied the influence of diverse heat treatments on the microstructural and tribological characteristics of Ti6Al4V ELI. No significant differences between the wear morphologies of the Ti6Al4V block surfaces were observed.

TABLE 2

Results of density, microhardness and compressive strength of spark plasma sintered Ti6Al4V

Temperature (°C)	1200		1300	
Compaction pressure (MPa)	25	50	25	50
Effective density (g/cm^3)	4.39 ± 0.04	4.39 ± 0.03	4.41 ± 0.02	4.44 ± 0.01
Microhardness ($HV_{0.05}$)	314 ± 2	295 ± 2	309 ± 5	295 ± 17
Compressive strength (MPa)	1153 ± 11	1159 ± 6	1150 ± 9	1166 ± 4

TABLE 3

Comparison of main friction and wear parameters (SD – standard deviation)

Parameter / Material	Block-on-Ring, (without lubrication)					Pin-on-Plate (bovine serum-lubrication)				
	Weight loss (mg)		R_a roughness of the blocks (μm)		Median friction coefficient (complete range)	Weight loss (mg)		Roughness R_a after the tests (μm)		Median friction coefficient (complete range)
	Block	Ring	Before	After		Plate	Pin	Plate	Pin	
SPS: 1200°C 25 MPa	77.8 (SD: 1.8)	9.8 (SD: 0.9)	0.43 (SD: 0.14)	3.01 (SD: 0.97)	0.33-0.40 (0.23-0.54)	-	-	-	-	-
SPS: 1200°C 50 MPa	76.8 (SD: 1.8)	9.5 (SD: 0.9)	0.20 (SD: 0.11)	3.99 (SD: 1.04)	0.36-0.40 (0.21-0.55)	-	-	-	-	-
SPS: 1300°C 25 MPa	74.7 (SD: 5.2)	11.7 (SD: 3.0)	0.15 (SD: 0.05)	2.68 (SD: 0.44)	0.34-0.40 (0.25-0.58)	-	-	-	-	-
SPS: 1300°C 50 MPa	72.9 (SD: 4.5)	9.16 (SD: 1.4)	0,13 (SD: 0.04)	2.21 (SD: 0.32)	0.34-0.36 (0.21-0.54)	0.0 (SD: 0.0)	0.072 (SD: 0.012)	0.05 (SD: 0.01)	0.29 (SD: 0.08)	0.052-0.063 (0.034-0.110)
Rod	-	-	-	-	-	0.0 (SD: 0.0)	0.069 (SD: 0.011)	0.05 (SD: 0.01)	0.24 (SD: 0.08)	0.039-0.041 (0.029-0.125)

Based on the preliminary testing results, Ti6Al4V sintered at the temperature of 1300°C under 50 MPa was chosen for further testing against UHMWPE, under bovine serum-lubrication. The weight loss of the Ti6Al4V plates despite the manufacturing process was negligible (TABLE 3). This is typical for metal-on-polyethylene articulation. It may also happen that the weight of the metal samples increases due to the transfer of polymeric material onto the metallic bearing surface [13]. The average weight loss for the UHMWPE pins articulating against the Ti6Al4V rod was slightly lower than UHMWPE articulating against the sintered Ti6Al4V (wear rate 7.36 mm^3/Nm and 7.67 mm^3/Nm respectively).

Fig. 4 illustrates the changes in the friction coefficient in relation to the number of running cycles for both the tested bearing couples: UHMWPE-on-Ti6Al4V rod – Fig. 4a and UHMWPE-on-sintered Ti6Al4V – Fig. 4b.

a)

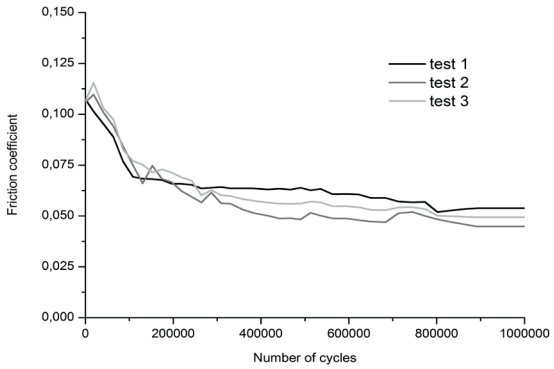

b)

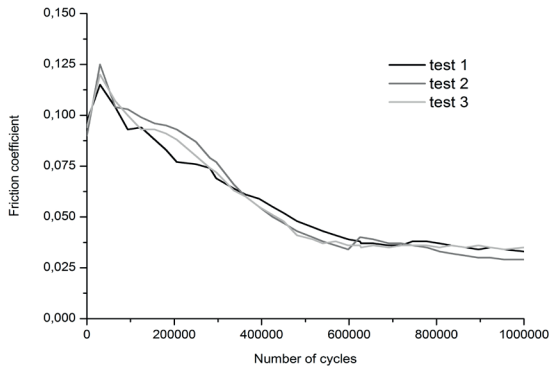

Fig. 4. Friction coefficient in relation to number of cycles for following bearing couples: a) UHMWPE articulating against Ti6Al4V rod; b) UHMWPE articulating against spark plasma sintered Ti6Al4V (bovine serum-lubrication)

As can be seen, the friction coefficient values start from high values for both kinds of bearing couples – it is the so-called run-in state. After about 500 000 (for sintered material) and after about 200 000 cycles (for rod material), the friction coefficient decreases to a steady state. A median friction coefficient for UHMWPE articulating against the sintered Ti6Al4V ranged between 0.039 and 0.041 (complete range 0.029-0.125) and against the Ti6Al4V rod ranged between 0.052 and 0.084 (complete range 0.045 - 0.121), which is very close to what may be found in the open literature data [14].

In the first stage of the test of the sintered Ti6Al4V-UHMWPE couple, the high friction coefficient might be explained by the greater initial roughness of the plates and more intensive machining of the pin. Progressive wear and transfer of UHMWPE debris onto the Ti6Al4V surface caused a local change of the type of articulation (polymer-on-metal replaced by polymer-on-polymer). The relatively low friction coefficient during the steady state for this bearing couple can be explained by the presence of open pores on the metal friction surface (Fig. 5a). The pores constitute a sort of local reservoirs for UHMWPE wear debris and bovine serum. On the surface of the reference material UHMWPE was also observed, but the nature of the presence was different. Polyethylene accumulated mainly in the wear scratches (Fig. 5b).

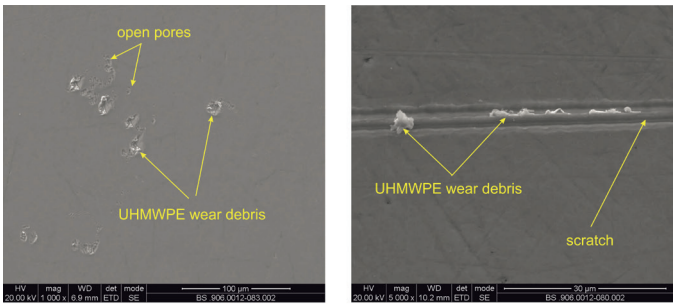

Fig. 5. Friction surface morphology: a) spark plasma sintered Ti6Al4V, b) Ti6Al4V rod

4. Conclusions

For the tested materials and sintering parameters applied in the present experiments, the following behavior was observed:

By changing the sintering parameters one can influence the size of the sintered Ti6Al4V grains.

The highest resistance to tribological wear was demonstated by the sample sintered at the temperature of 1300°C and compaction pressure of 50 MPa, and the smallest by the sample sintered at the temperature of 1200°C and compaction pressure of 25 MPa. It is associated primarily with the participation of various phases – as the presence of β increases, the wear resistant increases.

By comparing the wear resistance of the tested sintered materials and the elementary cell parameters - parameter c, it was noted that only in the case of the material sintered at the temperature of 1300°C and compaction pressure of 50 MPa was this value lower than the starting powder. The highest parameter c value was found for the sintered material with the lowest wear resistance. This relationship will be the subject of further analysis.

Using a sintered Ti6Al4V produced by the SPS method in combination with UHMWPE provides the opportunity to reduce the frictional resistance in a bovine serum environment compared to the UHMWPE-Ti6Al4V rod pair. It is necessary, however, to continue research in order to further optimize the structure in order to reduce the consumption of the cooperating polymer material - UHMWPE.

Acknowledgements

The studies were realized within the framework of statutory work BS 901 14 of the Metal Forming Institute in Poznan, entitled “Production of biocompatible composite materials for medical applications by the spark plasma sintering method (SPS)”.

REFERENCES

[1] Y. Quan, F. Zhang, H. Rebl, B. Nebe, Ol Kessler, E. Burkel, Materials Science and Engineering A **565**, 118, (2013).
[2] N. Biswas, J.L. Ding, International Journal of Impact Engineering **82**, 89 (2015).
[3] W. Shi, H. Dong, T. Bell, Materials Science and Engineering A **291**, 27 (2000).
[4] F. Zhang, M. Reich, O. Kessler, E. Burkel, Materials Today **16**, 192 (2013).
[5] S. G. Tabrizi, S. A. Sajjadi, A. Babakhani, W. Lu, Materials Science and Engineering A **624**, 271, (2015).
[6] H. Yanjun, L. Jinxu, L. Jianchong, L. Shukui, Z. Qinghe, Ch. Xingwang, Materials & Design **65**, 94, (2015).
[7] F. Despang, A. Bernhardt, A. Lode, Th. Hanke, D. Handtrack, B. Kieback, M. Gelinsky, Acta Biomaterialia **6**, 1006, (2010).
[8] J.W. Elmer, T.A. Palmer, S.S. Babu, W. Zhang, T. Debroy, Journal of Applied Physics 12 (2003).
[9] R. Pederson, O. Babushkin, F. Skystedt R. Warren, Material Science and Technology **19**, 1533 (2003).
[10] R. Dabrowski, Archives of Metallurgy and Materials **56**, 703, (2011).
[11] B. Vrancken, L. Thijs, J.P. Kruth, J. Van Humbeeck, Journal of Alloys and Compounds **541**, 177 (2012)
[12] I. Cvijović-Alagić, S. Mitrović, Z. Cvijović, D. Veljović, M. Barić, M. Rakin, Tribology in Industry **31**, 3-4, 17-22 (2009).
[13] M. Gierzyńska-Dolna, M. Lijewski, A. Mróz, Tribologia **3**, 255 (2014).
[14] J. Park, Bioceramic, Properties, Characterizations, and Applications, Springer Science+Business Media, New York 2008.